Differential expression of *PPP1R12A* transcripts, including those harbouring alternatively spliced micro-exons, in placentae from complicated pregnancies

Edward Frew [a], Rebecca Sainty [b], Louise Chappell-Maor [b], Caitlin Bone [b], Dagne Daskeviciute [b], Sarah Russell [b], Claudia Buhigas [b], Isabel Iglesias-Platas [c,d], Jon Lartey [a,e], David Monk [b,*]

[a] *Department of Obstetrics and Gynaecology, Norfolk and Norwich University Hospital NHS Foundation Trust, Norwich, UK*
[b] *Biomedical Research Centre, School of Biological Sciences, University of East Anglia, Norwich Research Park, Norwich, UK*
[c] *Neonatal Unit, Institut de Recerca, Sant Joan de Déu, Barcelona, Spain*
[d] *Neonatal Research, Norfolk and Norwich University Hospital NHS Foundation Trust, Norwich, UK*
[e] *Norwich Medical School, University of East Anglia, Norwich Research Park, Norwich, UK*

ARTICLE INFO

ABSTRACT

Introduction: Placenta-associated pregnancy complications, including pre-eclampsia (PE) and intrauterine growth restriction (IUGR) are conditions postulated to originate from initial failure of placentation, leading to clinical sequelae indicative of endothelial dysfunction. Vascular smooth muscle aberrations have also been implicated in the pathogenesis of both disorders via smooth muscle contractility and relaxation mediated by Myosin Light Chain Phosphatase (MLCP) and the oppositional contractile action of Myosin Light Chain Kinase. *PPP1R12A* is a constituent part of the MLCP complex responsible for dephosphorylation of myosin fibrils. We hypothesize that alternative splicing of micro-exons result in isoforms lacking the functional leucine zipper (LZ) domain which may give those cells expressing these alternative transcripts a tendency towards contraction and vasoconstriction.
Methods: Expression was determined by qRT-PCR. Epigenetic profiling consisted of bisulphite-based DNA methylation analysis and ChIP for underlying histone modifications.
Results: We identified several novel transcripts with alternative micro-exon inclusion that would produce LZ-PPP1R12A protein. qRT-PCR revealed some isoforms, including the *PPP1R12A* canonical transcript, are differentially expressed in placenta biopsies from PE and IUGR samples compared to uncomplicated pregnancies.
Discussion: We propose that upregulation of *PPP1R12A* expression in complicated pregnancies may be due to enhanced promoter activity leading to increased transcription as a response to physiological stress in the placenta, which we show is independent of promoter DNA methylation.

1. Introduction

The placenta is a temporary organ that allows direct contact between the developing fetus and the uterus during pregnancy. In addition to producing hormones to ensure continuation of development during the first weeks of pregnancy, it becomes the route of oxygen, glucose and nutrient exchange from mother to fetus, as well as enabling the diffusion of metabolic waste products and carbon dioxide from fetal blood [1]. This exchange between bloodstreams occurs without the fetal and maternal blood mixing. Placenta blood vessel remodelling is key to successful pregnancy. This begins when placental trophoblasts invade

spiral arteries during the first week of pregnancy, modifying the arteries from low-flow, high-resistance to high-flow, low-resistance vessels capable of meeting the metabolic demands of the developing fetus [2]. Therefore, the maternal-placenta vessel architecture is important in dictating pregnancy success. Patients with pre-eclampsia (PE) and intrauterine growth restriction (IUGR) frequently have compromised uteroplacental artery remodelling, partly due to shallow trophoblast invasion, leading to attenuated blood flow in the uterine arteries evidenced as abnormal pulsatility index in umbilical artery Doppler velocimetry [3,4]. Pathways involved in regulating trophoblast and vessel physiology are excellent candidates for understanding the molecular mechanisms involved in the aetiology of PE and IUGR. The gene

PPP1R12A (also known as *MYPT1*) encodes a protein expressed in placenta trophoblasts, endothelial cells and smooth muscle of blood vessels (The Human Protein Atlas portal https://www.proteinatlas.org/)) and has been implicated in uterine contractions during labour [5]. PPP1R12A encodes a >110 kDa protein phosphate 1 regulatory subunit and is a key regulator of the protein phosphatase 1c (PP1c), part of the myosin light chain phosphatase holoenzyme that is responsible for relaxation in smooth muscle cells [6]. Nitric oxide (NO)-mediated smooth muscle relaxation is partly attributed to activation of the phosphatase by protein kinase G (PKG) binding to a leucine zipper (LZ) dimerization domain located in the C-terminal region of PPP1R12A [7]. Several studies have reported that alternative splicing of a 31-base pair (bp) micro-exon results in a frameshift event generating a LZ negative (LZ-) transcript that is less sensitive to NO and PKG binding [5,8–10]. Therefore, the LZ positive (LZ+) and LZ-isoforms may possess different phosphatase activities that ultimately influence smooth muscle contractility and cellular function.

With the advent of RNA-seq which generates unbiased transcriptomes, there is now the prospect of detecting previously undiscovered transcripts, produced via alternative splicing, a mechanism which enables multiple isoforms to be produced from a single gene. The inclusion of small sized exons of <51 bp, termed micro-exons, has been shown to influence cellular physiology and disease, especially in brain [11–13]. The human genome is estimated to contain more than 13,000 highly conserved micro-exons, many of which exhibit differential expression between tissues [14]. Through bioinformatic analysis and molecular confirmation, we identify multiple alternative splicing events of 3′-derived micro-exons that all result in *PPP1R12A* LZ-variants that show varying abundance in term placenta. Although we do not find differential inclusion of all LZ-variants in placenta biopsies from complicated pregnancies, we do observe that several *PPP1R12A* transcripts are differentially expressed in pre-eclampsia, being up-regulated, in a DNA methylation independent manner.

2. Materials and methods

2.1. Sample cohort

Women delivering their babies in Sant Joan de Déu Hospital, Barcelona Spain or Norfolk and Norwich University Hospital, UK were recruited and participated in the study following individual informed consent. The study protocol was approved by the Ethics Committee of Sant Joan de Déu Hospital and NRP Biorepository Access Committees (PI35/07 and BAC.010.22). Control placental samples were obtained from donors delivering at term (≥37 weeks), late and moderate preterm (>32 and < 37 weeks) and very preterm (≤32 weeks) (n = 18). Samples were also obtained from donors whose pregnancies were complicated by IUGR (n = 18), defined as a weight below the 3rd percentile for gestational age or below the 10th percentile when accompanied by fetal Doppler flow abnormalities and PE (n = 18) defined as hypertension (systolic ≥160 mm Hg and/or diastolic of ≥100 mm Hg) proteinuria and any of the following clinical sequelae: thrombocytopenia, impaired liver function, renal insufficiency, pulmonary edema and unexplained new-onset, unresponsive headache or visual disturbances. After delivery, the placentae were weighed and biopsies from the fetal side 5 cm from the umbilical cord insertion site were excised (Supplementary Table 1). The tissue was thoroughly rinsed in saline and snap frozen in liquid nitrogen. Paired placental blood vessels and villous samples were microdissected using a Leica S8AP0 microscope and samples snap frozen in liquid nitrogen. First trimester placenta samples were obtained from the MRC-Wellcome Trust Human Developmental Resource (HDBR).

2.2. Cell lines

The endothelial cell line HMEC-1 and two trophoblasts lines, TCL1 and SWAN71, were propagated using standard aseptic cell culture techniques. HMEC-1 were cultured using MCBD-131 medium supplemented with 10 % fetal calf serum (FCS), 2 % penicillin-streptomycin, L-glutamine (10 mM), hydrocortisone (0.1 μg/ml) and endothelial cell growth supplement (10 ng/ml). Both trophoblast lines were cultured in DMEM media supplemented with 10 % fetal calf serum (FCS), 1 % penicillin-streptomycin, L-glutamine (10 mM). All lines were cultured at 37 °C in a 5 % humidified atmosphere.

2.3. Nucleic acid extraction

Processing of placenta samples has been described previously [15]. Genomic DNA was prepared by SDS/Proteinase K lysis followed by phenol/chloroform extraction and ethanol precipitation. Total RNA was extracted using Trizol® (Invitrogen), and 1 μg of RNA was treated with DNase (amplification grade DNase I, Invitrogen) prior to reverse transcription. Reverse transcription was performed with MMLV reverse transcriptase (Promega) and random primers (Promega) following the manufacturer's instructions. Total RNA and DNA from normal uterus samples were purchased from Biochain.

2.4. Quantitative polymerase chain reaction

Expression of *PPP1R12A* isoforms was analysed by quantitative real-time RT-PCR with a fluorochrome (SYBR® Green) assay and normalized against the average of *ACTB* and *RPL19* [16] (Table 1 for primer sequences). The assays were run in triplicate in 384 well plates in QuantStudio 5 Real-Time PCR system (Applied Biosystems). Dissociation curves were obtained at the end of each reaction to rule out the presence of primer dimers or unexpected DNA products in the reaction. Non-template controls, an interplate control and standard curves from the same serial dilutions of cDNA obtained from pooled normal placental tissue were included in each assay. Results were analysed with the SDS 2.3 software (Applied Biosystems). The DataAssist v2.0® software (Applied Biosystems) was used for exclusion of outlier replicates and for interplate standardization for comparisons. Only samples with two or more valid readings per triplicate were included. Analysis of the results was performed using the comparative ΔΔCT relative quantification (RQ) method [17].

2.5. Standard bisulphite PCR

Approximately 1 μg DNA was subjected to sodium bisulphite treatment and purified using the EZ GOLD methylation kit (ZYMO) with ~50 ng of converted DNA used for all bisulphite PCR reactions. Bisulphite PCR primers for each region were used with Immolase Taq polymerase (Bioline) at 45 cycles with an annealing temperature of 53 °C (see Table 1 for primer sequences). The resulting PCR product was cloned into pGEM-T easy vector (Promega), transfected into JM109 bacteria and individual colonies were sequenced using standard T7 sequence primer.

2.6. Methylation analysis by bisulphite pyrosequencing

1 μg of DNA was subject to bisulphite conversion using the EZ Gold kit in a 96-well plate format (EZ-96 DNA Methylation-Gold™® Kit,

Table 1
Oligonucleotide PCR primers used in this study.

Primer	Sequence (5′-3′)	Annealing temp (ºC)	Size
Common F	GACAAGAAAGATTTGCTGATAG	60	
Wild type R	TAGAGCTCTTCGTTCCCTTTTTT	60	62 bp
13 bp micro-exon R	AGCTCTTCGTTCTCTTGCCGGTC	60	72 bp
31 bp micro-exon R	AGCTCTTCGTTCCGCCCAGAAGA	60	90 bp
Readthrough R	AGCATTCTGGGGTGTTATGCAA	60	148 bp
4 bp micro-exon F	CTTCTTTCTAGAGCTCTTGGATC		
4 bp micro-exon R	AACCTTACAGCAGCAGGCTAGAA	60	226 bp
RPL19 qRT-PCR F	AATCGCCAATGCCAACTCCCGTCA		
RPL19 qRT-PCR R	CCTATGCCCATGTGCCTGCCTTC	60	133 bp
ACTB qRT-PCR F	CCGGCTTCGCGGGCGACGAT		
ACTB qRT-PCR R	CTCCATGTCGTCCCAGTTGG	60	194 bp
PPP1R12A bisulphite F	TAGGGGGTGTGTGAATGTTTTTAT		
PPP1R12A bisulphite R	CTCCTTTCCAAATCTATCCCAACC	53	360 bp
PPP1R12A ChIP F	CCACATTGGCGTAATTGATGTC		
PPP1R12A ChIP R	AAGCGCCAGAAGACCAAGGTGA	60	127 bp
SNURF:TSS-DMR ChIP F	CTGTGCTACTGCCCCTTCTG		
SNURF:TSS-DMR ChIP F	GGAGTGACTAAGGGACGCTGAATG	60	68 bp

Zymo Research), following the manufacturer's protocol and 2 μl used per PCR. Pyrosequencing was selected for the quantitative assessment of DNA methylation at the *PPP1R12A* promoter with the exception that the reverse primer was biotin-labelled. Immobilization of the PCR products for purification was achieved by streptavidin-coated sepharose beads (Qiagen) with the use of the PyroMark Q96 Vacuum Prep Workstation® and sequenced using a PyroMark Q96 MD machine according to the manufacturer's instructions.

2.7. Western blotting

Protein samples were extracted using the Dignam protocol (Buffer A-C) and the resulting cytoplasmic and nuclear fractions mixed in equal amounts. After determination of protein concentration using Nanodrop, equal amounts of total proteins were resolved using 10 % SDS-PAGE. Afterward, the electrophoretic transfer of proteins onto polyvinylidene fluoride membranes was performed, with efficient transfer confirmed using Ponceau S staining, followed by probing with antibodies against ACTB (α-Actin-HRP Sigma #A3854, 1:10,000 dilution), PPP1R12A (α-MYPT1 ProteinTech #22117-1-AP, 1:10,000 dilution) and secondary antibody conjugated with horseradish peroxidase (α-rabbit-IgG-HRP, Sigma #A0545,1:200 dilution). Targeted bands were detected using an enhanced chemiluminescence detection system.

2.8. Chromatin immunoprecipitation

Material for chromatin immunoprecipitation (ChIP) was from samples described previously [18,19]. Briefly, 4 μg of chromatin in a total volume of 500 μL were used for each condition. Precleared chromatin was incubated with antibodies-beads complexes for 4 h at 4 °C using antibodies directed against H3K4me3 (Diagenode C15410003-50), H3K4me2 (Millipore 07–030), H3K9ac (Cell Signaling 9649S), H3K9me3 (Abcam AB8898), H3K9me2 (Diagenode C15410060) and a negative control (mock precipitation with mouse IgG Millipore 12–371). The antibody-chromatin complexes were washed and only the fraction of chromatin linked to the antibodies was retained. The eluted DNA was obtained from the input and bound fractions following Nucleospin gel and PCR clean-up (Macherey-Nagel), according to the manufacturer's protocol ready for qPCR.

2.9. Statistical analysis

Clinical and molecular data were introduced in a Statistical Package for Social Sciences (SPSS) software v17.0 database. Expression levels were expressed in logarithmic scale in order to achieve a variable distribution closer to normality and subsequently analysed against clinical values. Comparisons between groups for clinical data were evaluated with chi-square for categorical variables and *t*-Student test (for two groups, 2-tailed analysis) or ANOVA (more than two groups) for continuous variables. Non-parametric tests were applied where indicated. For qRT-PCR difference in mean expression between groups was determined using Wilcoxon signed-rank test. Results were considered significant if the p-value was under 0.05; values under 0.1 were considered as a trend. Figures were produced using in-house R scripts.

2.10. RNA-seq analysis

RNA-seq data from placenta sample collected across gestation (PRJEB38810) were used in order to identify the alternatively spliced micro-exons. Raw reads were aligned using STA in 2-pass mode to extract splice junctions. The splice junctions are then inserted in the reference genomic index and all reads are re-mapped. Alignments were assembled into transcripts with StringTie 2.0.6.

3. Results

3.1. Characterising alternatively spliced LZ-isoforms

We have previously reported the alternative splicing of *PPP1R12A* can lead to the inclusion of a 31 bp micro-exon that generates a LZ-isoform rendering the phosphatase less sensitive to NO vasodilators in uterine smooth muscle [5]. In order to determine if alterations in LZ+/LZ-ratios are linked to pregnancy complications in placenta samples, we interrogated *PPP1R12A* mRNA/Expressed Sequence Tags (ESTs) sequences to see if any novel transcripts were present that would result in a LZ-protein (Fig. 1A). Visual inspection of intron 23 of *PPP1R12A* (reference transcript NM_002480.2) using the UCSC genome browser revealed several different micro-exons that would all result in open reading frame frameshifts generating *PPP1R12A* isoforms that are LZ-. One of these isoforms resulted from alternative 3' splice donor site resulting in a 13 bp (CA390922) micro-exon overlapping the aforementioned 31 bp (BM669210) variant. Furthermore, intron retention (readthrough transcript) immediately following the inclusion of these micro-exons also resulted in a predicted LZ-isoform (AK125671). Approximately 650 bp upstream of the 13–31 bp micro-exon sequence is another annotated 4 bp alternatively spliced micro-exon (BE302367), which would also produce an LZ-variant, although the precise location of the TAGG sequence is unknown as there are eight tetra-nucleotide sequences within intron 23 of *PPP1R12A*. To determine if these alternatively spliced variants are detectable in term placenta and uterus, we performed RT-PCR validation experiments using isoform-specific primers designed across splice sites or within unique transcript sequences, followed by Sanger sequencing. This confirmed the inclusion of all micro-exons and the readthrough transcript (Fig. 1A and B). The absolute expression levels were subsequently determined in placenta biopsies and micro-dissected blood vessels using quantitative RT-PCR. Total PPP1R12A proteins levels were investigated with western blotting. Consistent with the frequency of mRNA/EST transcripts in UCSC Genome browser, the canonical isoform (NM_002480) was the most
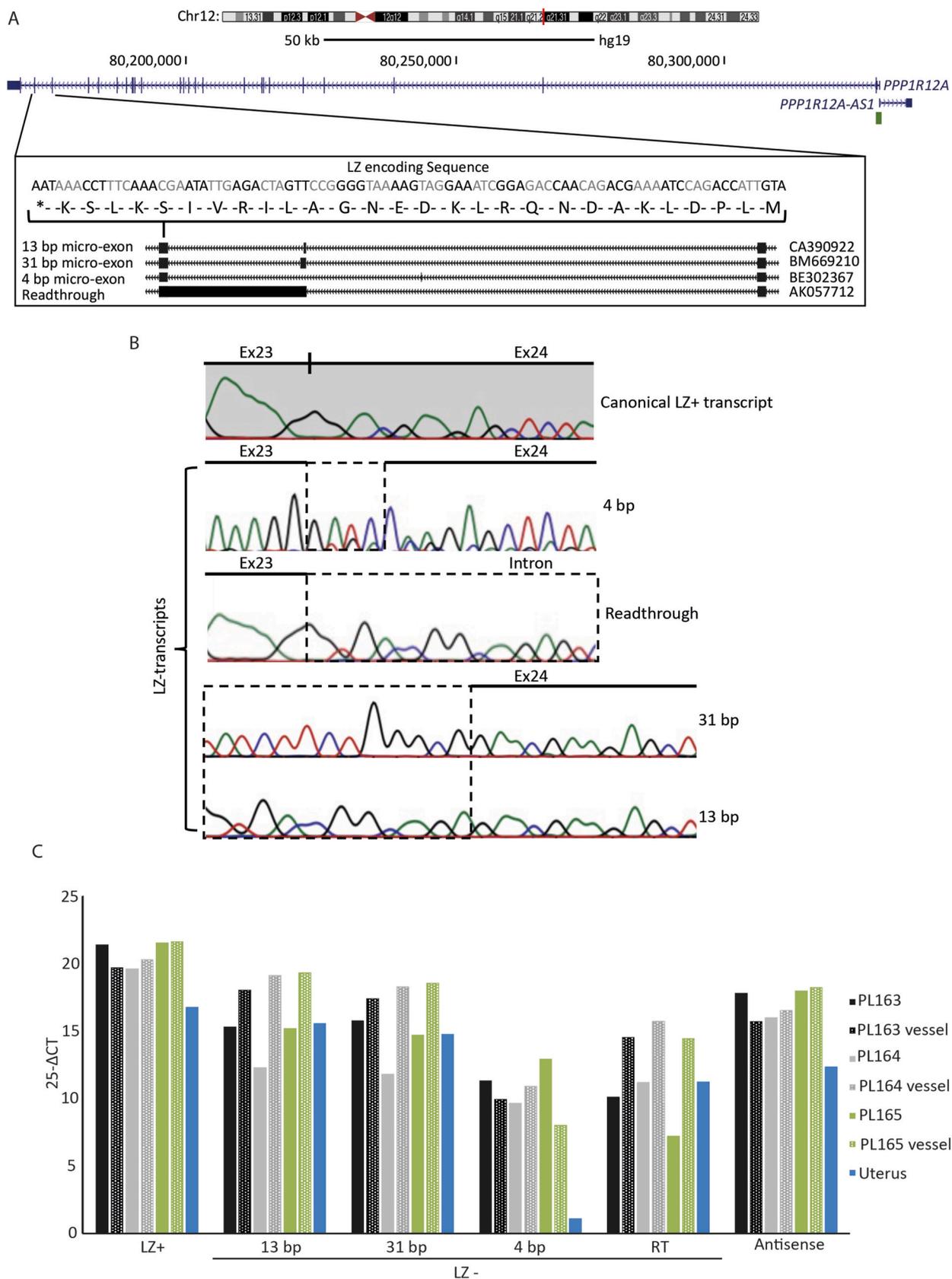
Fig. 1. Schematic overview of the *PPP1R12A* locus on chromosome 12. (A) The entire regions showing the orientation of the *PPP1R12A* and *PPP1R12A-AS1* transcripts, as well as the promoter CpG island (green). The insert is a focal view point of intron 23 showing the position of the micro-exons and read-through transcripts. Arrows indicate the direction of transcription. (B) Sanger sequencing of isoform-specific RT-PCR amplicons incorporating the LZ-micro-exon or read-through sequences. (C) Bar graphs showing the relevant *PPP1R12A* isoform abundance in paired placenta vessel and villous samples, as well as uterus.

abundant, followed by 13 and the 31 bp micro-exons transcripts, with the 4 bp and readthrough variants being reproducibly lowly expressed (Fig. 1C). The readthrough and micro-exon containing transcripts showed the most variability between placenta and their paired vessels compared to canonical LZ + transcript. Pan PPP1R12A protein expression was observed across gestation, albeit more abundant in term samples compared to first trimester and the protein was observed in endothelial and trophoblast cell lines (Supplementary Fig. 1). Interrogation of first trimester and term placenta RNA-seq datasets was largely inconclusive. Using the splice aware aligner STAR, we only observe the 31 bp micro-exon and the readthrough transcript. Presumably the datasets were sequenced to insufficient depth to allow for the detection of the other micro-exons. Alternatively, the use of weak splice donor sites, exemplified by the 13 bp micro-exon which utilised a cytosine at +3 position that is only present in 3 % of splicing events, resulted in inefficient calling of these micro-exons compared to splicing events using the stronger canonical splice junction sequences (Supplementary Fig. 2).

3.2. Expression of PPP1R12A micro-exons in placenta samples complicated by PE and IUGR

We analysed the relative mRNA transcript levels for five *PPP1R12A* isoforms described above in human placentae by qRT-PCR in comparison to the endogenous *RPL19* and *ACTB* housekeeping genes. Expression of the canonical *PPP1R12A* LZ + isoform was higher in samples in both the IUGR (p = 0.031) and PE (p = 0.007) groups compared to gestational aged-matched controls (Fig. 2A). Similar profiles were observed when all isoforms were examined together (Fig. 2B). The expression of the 4 bp micro-exon containing transcript was elevated in the PE cohort compared to the other groups (p = 0.02) (Fig. 2C). The 13 bp *PPP1R12A* LZ-isoform was more abundant on both the IUGR and PE groups (Fig. 2D). The expression of the readthrough and 31 bp micro-exon isoforms were invariant in the control, PE and IUGR groups (p > 0.05) (Fig. 2E and F). Our analysis confirms that the difference in *PPP1R12A* LZ-isovariant expression in PE and IUGR cohorts is predominantly due to changes in the expression of the 4 bp and 13 bp and not the
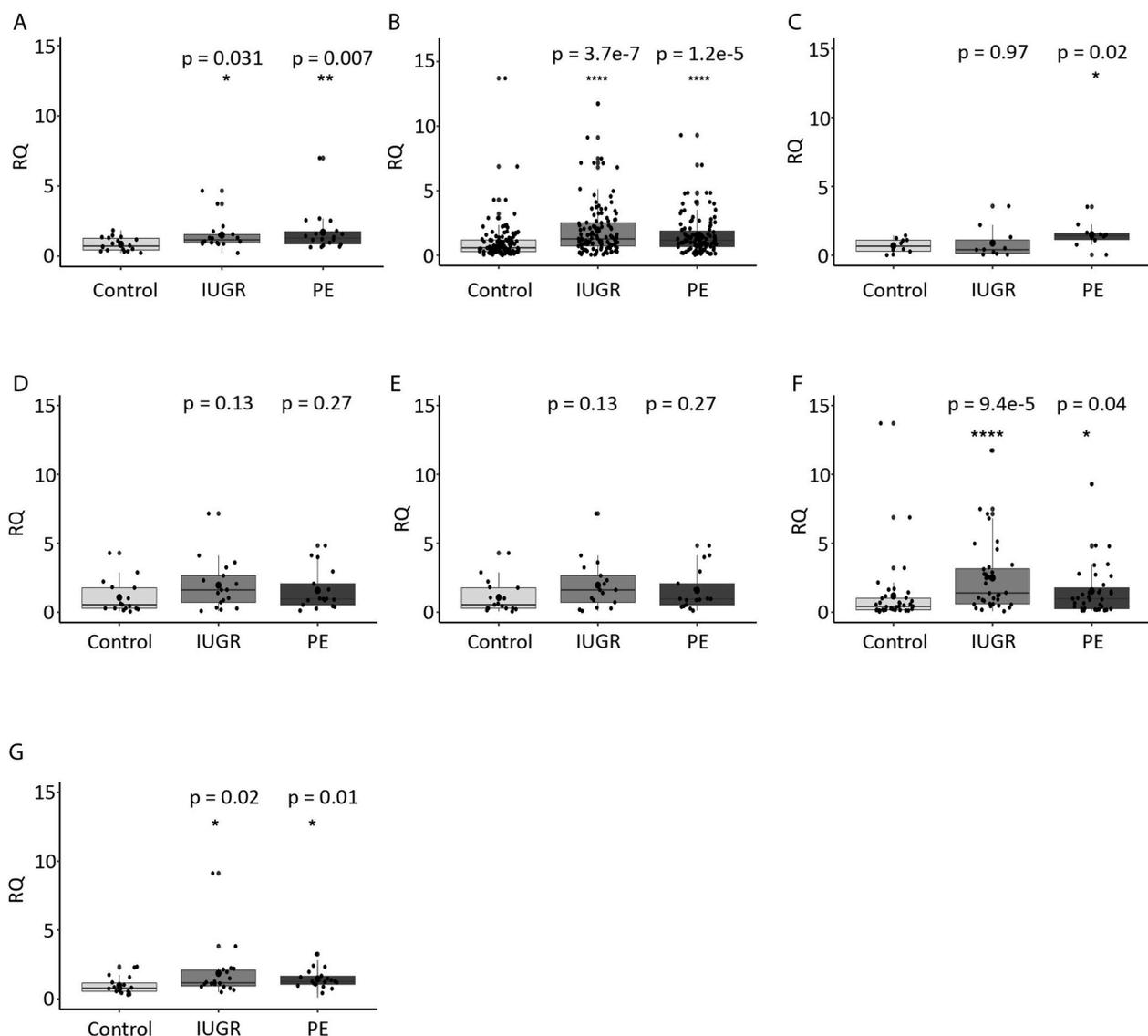
Fig. 2. Expression profiling of the *PPP1R12A* transcript isoforms in placenta biopsies from complicated pregnancies. Quantification of expression levels of (A) WT, (B) all isoforms, (C) 4 bp micro-exon, (D) the read-through, (E) 31 bp micro-exon, (F) the 13 bp micro-exon and (G) the *PPP1R12A-AS1* transcript in control, IUGR and PE samples (n = 18 per group) by qRT-PCR. The results are presented as box plots, with individual data points (black dots) shown. All expression levels were normalized to the average of *ACTB* and *RPL19* housekeeping genes. To determine the statistical significance of the difference between the IUGR/PE and control groups, Wilcoxon signed-rank test was used and p values are indicated for each comparison.

readthrough and 31 bp isoforms.

3.3. Epigenetic characterisation of the PPP1R12A promoter interval

Our analysis confirms the differential expression of both LZ+ and some LZ-isoforms was observed in samples from complicated pregnancies compared to controls (Fig. 2A and B), indicating that aberrant micro-exon inclusion is not the only mechanism responsible for the phenotypes observed, but that upregulation of transcription from the promoter interval maybe important. To determine if there are epigenetic changes that could be responsible for the change in total gene abundance observed, we first profiled the DNA methylation and post-
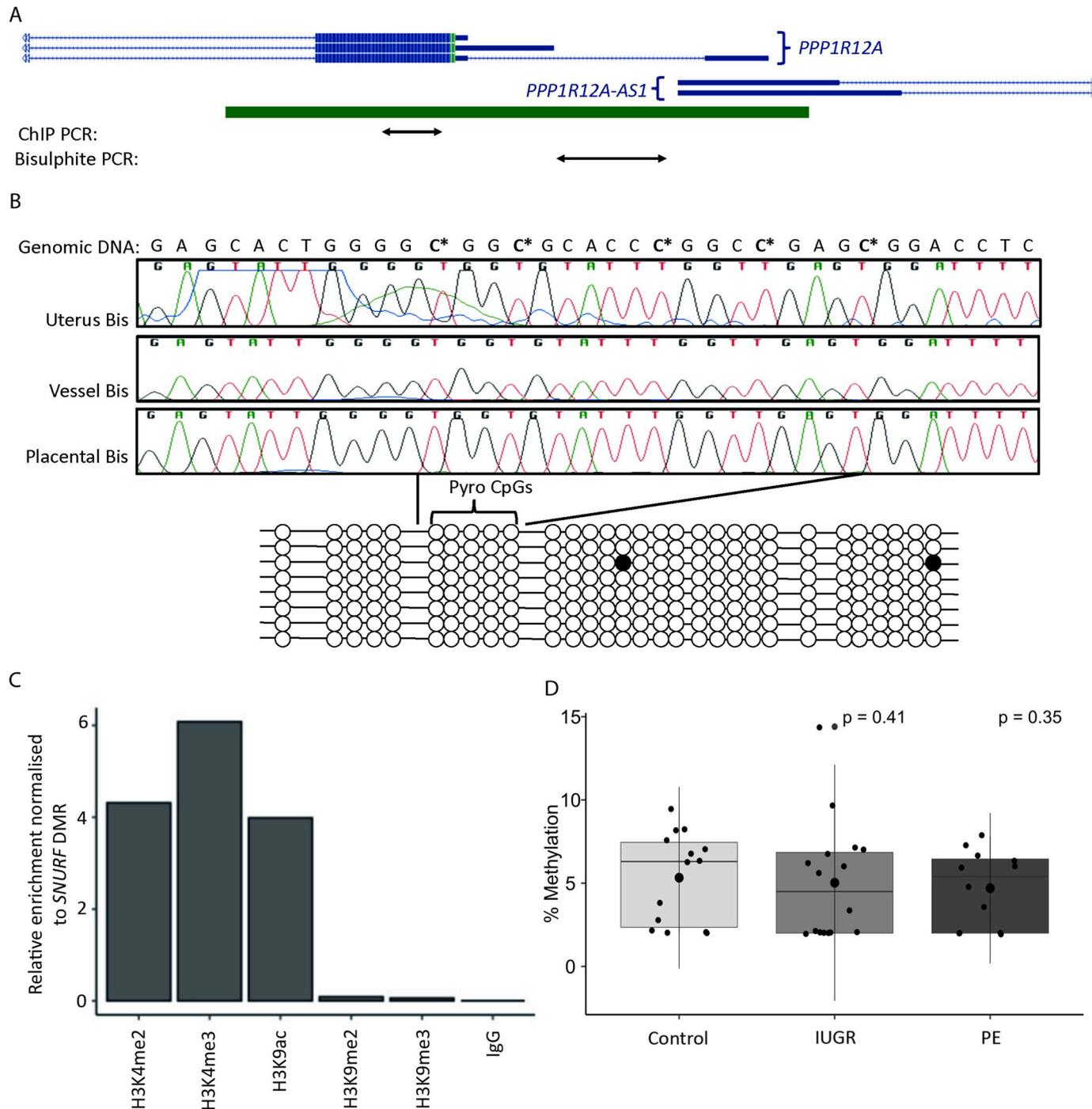
Fig. 3. Epigenetic analysis of the *PPPIR12A* promoter interval. (A) Schematic overview of the promoter interval showing the location of the CpG island and primers used for ChIP and bisulphite PCR. (B) Characterization of the promoter CpG islands in uterus, blood vessel and placenta-derived DNA samples. The Sanger sequence tracks show the location of selected unmethylated CpG positions before cloning of the PCR amplicons. The entire DNA methylation profile is shown for the placenta PCR product following cloning of individual DNA strands. Each circle represents a single CpG on a DNA strand. (●) methylated cytosine, (o) unmethylated cytosine. Each row corresponds to an individual cloned sequence. (C) Quantitative PCR on ChIP material. Precipitations were normalized to the SNURF promoter since opposing alleles have active/repressive histone modification profiles. The graphs represent the mean values of triplicate PCRs. (D) Pyrosequencing quantification of the *PPP1R12A* promoter. The violin plots include the mean (black dots). To determine the statistical significance of the difference between the IUGR/PE and control groups (n = 18 per group), Student's two-tailed t-test was used, and p values are indicated for each comparison.

translational histone modification signatures in control samples. Using bisulphite PCR and sub-cloning we characterised the DNA methylation of the CpG island that overlaps the two transcriptional start sites for the *PPP1R12A* and an antisense non-coding transcript (Fig. 3). Consistent with a more permissive epigenetic state within the promoter interval, *PPP1R12A-AS1* (DB045059) was also differentially expressed in IUGR (p = 0.02) and PE (p = 0.01) placenta samples compared to controls (Fig. 2G). In placenta, micro-dissected blood vessels and uterus-derived DNA samples, this interval encompassing thirty CpG dinucleotides, was robustly unmethylated (Fig. 3A and B).

We subsequently characterised markers of both active and repressive chromatin states in three control placenta samples. Chromatin immunoprecipitation using antibodies raised against the permissive histone modification di-methylation of lysine 4 of histone H3 (H3K4me2), H3K4me3 and acetylation of lysine 9 of histone H3 (H3K9ac), as well as the heterochromatic marks H3K9me2 and H3K9me3 was employed and precipitation levels compared to known loci enriched for these modifications [18]. This revealed that the promoter interval of *PPP1R12A* is decorated with the active modifications, especially H3K4me3 and H3K9ac, but depleted for the repressive H3K9 methylation states, consistent with the lack of CpG DNA methylation and heterochromatic state (Fig. 3C).

3.4. Normal DNA methylation of the PPP1R12A promoter in IUGR and PE

To determine if the differences in expression observed in IUGR and PE are due to changes in DNA methylation at the *PPP1R12A* promoter we performed pyrosequencing to quantify methylation levels. Using the same bisulphite PCR assay described above, we quantified five CpG dinucleotides using an internal sequence primer. The arithmetic mean of these CpG dinucleotides was used as a representative measure of the level of methylation for each placenta sample in our cohort. Pyrosequencing confirmed the *PPP1R12A* promoter is hypomethylated, revealing no significant differences between control and IUGR or PE placentae (mean % methylation 5.3 ± 2.7 SD in controls vs. 5.0 ± 3.5 SD in IUGR, Student's t $p = 0.41$ and 4.7 ± 2.3 SD in PE, Student's t $p = 0.35$) (Fig. 3D).

4. Discussion

Alternative splicing has major influence in regulating the proteome, resulting in the synthesis of different protein variants from the same gene. In many cases, alternative exon usage can regulate structural domain composition of a protein [20]. Different splicing isoforms, including those involving micro-exons, can lead to changes in reading frame, resulting in the generation of divergent protein isoforms that may have opposing function, as well as influencing protein-protein interactions and cellular localisation. For example, alternative splicing of *RBFOX1* leads to differential protein localisation within the cell, with transcripts excluding exon 19 preferentially found in the nucleus, whereas those including exon 19 are found in the cytoplasm [21]. RBFOX1 itself encodes an RNA-binding splicing factor, which when depleted in neurones significantly changes the exon inclusion of >500 mRNAs [22]. Previous reports have suggested that only ~40 % of micro-exon inclusions preserve the mRNA reading frame, whereas the majority introduce premature stop codons or induce nonsense-mediated mRNA decay [23].

Here we present evidence of three *PPP1R2A* LZ-isoforms including 4 bp, 13 bp and the classical 31 bp isovariants in human placental vessels and tissue samples. Our analysis confirms an upregulation of the expression of 4 bp and 13 bp micro-exon containing *PPP1R12A* LZ-isoforms in pregnancies complicated by PE and fetal growth restriction. We have previously demonstrated the expression of *PPP1R12A* LZ+ and a 31 bp micro-exon LZ-isoform in myometrial and placental vessels and tissue samples [5]. This is the first report demonstrating the expression of the 4 bp and 13 bp micro-exon LZ-isoforms in human placental samples, which presumably encode proteins with similar function, being less sensitive to NO and PKG binding. The expression of the 31 bp LZ-isoform was similar in the control, PE and IUGR groups, whereas the expression of the *PPP1R12A* LZ + isoform was elevated in the IUGR and PE groups compared to control group. Other investigators have suggested exon 24 can be spliced in two different ways with inclusion of either a 13 and 31 bp and we now present inclusion of a 4 bp mini-exon which can also generate a LZ-isovariant [10].

The expression of LZ + or LZ-isoforms are developmentally regulated and appear to be tissue specific. For instance, tonic contraction smooth muscle tissues like the aorta express the exon excluded LZ + isoform whereas phasic smooth muscle organs like gizzard and bladder express the LZ- [24–27]. The expression of *PPP1R12A* LZ isoforms can be modified in certain vascular disease states raising the possibility that alternative splicing may be an adaptive response to a pathological insult like abnormal placental blood flow. A rat disease model monitoring the effect of chronic low and high blood flow demonstrated an initial global reduction in *PPP1R12A* expression and switch to LZ + isoform. However, long-term chronic blood flow was characterised by a change to LZ-isoform whilst low blood flow vessels maintained LZ + phenotype and sensitivity to vasodilators [28]. An animal model of congestive heart failure demonstrated reduction in LZ + isoforms expression and tissue sensitivity to 8 bromo-cGMP (8-Br-cGMP) in diseased compared to control rats, confirming that tissue resistance to nitric oxide induced vasodilation is due to a loss of the LZ + isoform [29,30]. Variation in alternative splicing exon 24 generating LZ + or LZ-isoforms seems to be largely isolated to specific smooth muscle cells and only accounts for 6 % of *PPP1R12A* isovariant expression in platelets and is rarely seen in human umbilical vein endothelial cells or saphenous vein smooth muscle cells [10].

The significant increase in the expression of specific LZ-isoforms in PE and fetal growth restriction cohorts presented above is consistent with altered vascular tissue resistance to vasodilators in this high resistance disease state and can explain the lack of response to nitric oxide dependent vasodilators in modulating tissue tone and neonatal outcome outlined by previous investigators [31]. Sildenafil, a nitric oxide donor, did not prolong pregnancy or improve fetal weight at delivery, live birth rates or reduce fetal or neonatal deaths [32]. Interestingly, sildenafil use was associated with modest short-term reductions in maternal pulse, blood pressure and arterial stiffness suggesting its lack of effect on placental haemodynamics and fetal and neonatal outcomes may be organ-specific and due to the disease associated phenotype increase in placental LZ-isoform expression and an attenuation of tissue responsiveness to calcium sensitising agonists and nitric oxide dependent vasodilators [33]. These changes in *PPP1R12A* LZ-isovariant expression in these complicated pregnancies are consistent with an overall switch from slow-tonic to a fast-phasic contractile phenotype outlined in an animal model of congestive heart failure [34].

The PPP1R12A subunit is also present in the human uterus, a smooth muscle organ capable of both tonic and phasic contractile activity required for labour [35,36]. Hudson and colleagues elegantly outlined agonist induced phasic contractile activity in the human uterus is mediated via kinase phosphorylation of PPP1R12A subunit at Thr853 and myosin at Thr18/Ser19 [37]. We later demonstrated a decrease in the expression of both PPP1R12A LZ+ and LZ-isoforms from donors in labour compared to pregnant not in labour and non-pregnant donors [5]. Dordea et al. presented similar levels of *PPP1R12A* LZ+ and LZ-in human myometrial and placental arteries but with higher levels of 8-Br-cGMP induced relaxation in myometrial arteries suggesting alternative regulators with alternative splicing and LZ isovariant expression [38]. This reduction in 8-Br-cGMP/NO relaxation in placental arteries is associated with a reduction on myofilamental contractile protein HSP20.

Overall, our targeted qRT-PCR approach has revealed the complexities of *PPP1R12A* LZ+ and LZ-abundance in placenta. To determine the

absolute abundance of each of the alternatively spliced isoforms in target cells, future work should incorporate the integration of short- and long-read sequencing approaches in cells isolated from different placenta and myometrial biopsies in normal and complicated pregnancies to help understand the complexity in cellular transcription and function in this unique developmental tissue. Furthermore, future studies should aim to quantifying total LZ+ and LZ-protein abundance, thus allowing a ratio in samples from complicated pregnancies to be determined, which is not possible at the current time due to the lack of suitable C-terminal antibodies.

Funding

CRediT authorship contribution statement

Edward Frew: Conceptualization, Data curation, Writing – original draft, Writing – review & editing. **Rebecca Sainty:** Writing – original draft, Writing – review & editing, Data curation. **Louise Chappell-Maor:** Conceptualization, Data curation, Methodology, Writing – original draft, Writing – review & editing. **Caitlin Bone:** Methodology, Writing – review & editing. **Dagne Daskeviciute:** Conceptualization, Data curation, Writing – original draft, Writing – review & editing. **Sarah Russell:** Data curation, Writing – original draft. **Claudia Buhigas:** Data curation, Writing – original draft, Writing – review & editing. **Isabel Iglesias-Platas:** Data curation, Resources, Writing – original draft. **Jon Lartey:** Funding acquisition, Resources, Supervision, Writing – original draft, Writing – review & editing, Conceptualization. **David Monk:** Funding acquisition, Resources, Writing – original draft, Writing – review & editing.

Declaration of competing interest

The authors declare that they have no known competing financial interests or personal relationships that could have appeared to influence the work reported in this paper.

Acknowledgements

Appendix A. Supplementary data

Supplementary data to this article can be found online at https://doi.org/10.1016/j.placenta.2024.04.005.

References

[1] E. Maltepe, S. Fisher, Placenta: the forgotten organ, Annu. Rev. Cell Dev. Biol. 31 (2015) 523–552, https://doi.org/10.1146/annurev-cellbio-100814-125620.

[2] R. Pijnenborg, L. Vercruysse, M. Hanssens, The uterine spiral arteries in human pregnancy: facts and controversies, Placenta 27 (2006) 939–958, https://doi.org/10.1016/j.placenta.2005.12.006.

[3] S. Rana, E. Lemoine, J. Granger, S. Karumanchi, Preeclampsia: pathophysiology, challenges, and perspectives, Circ. Res. 124 (2019) 1094–1112, https://doi.org/10.1161/CIRCRESAHA.118.313276.

[4] G. Burton, E. Jauniaux, Pathophysiology of placental-derived fetal growth restriction, Am. J. Obstet. Gynecol. 218 (2018) S745–S761, https://doi.org/10.1016/j.ajog.2017.11.577.

[5] J. Lartey, J. Taggart, S. Robson, M. Taggart, Altered expression of human smooth muscle myosin phosphatase targeting (MYPT) isovariants with pregnancy and labour, PLoS One 11 (2016) e0164352, https://doi.org/10.1371/journal.pone.0164352.

[6] J. Lartey, A. López Bernal, RHO protein regulation of contraction in the human uterus, Reproduction 138 (2009) 407–424, https://doi.org/10.1530/REP-09-0160.

[7] A. Given, O. Ogut, F. Brozovich, MYPT1 mutants demonstrate the importance of aa 888-928 for the interaction with PKGI alpha, Am. J. Physiol. Cell Physiol. 292 (2007) C432–C439, https://doi.org/10.1152/ajpcell.00175.2006.

[8] W. Dirksen, F. Vladic, S. Fisher, A myosin phosphatase targeting subunit isoform transition defines a smooth muscle developmental phenotypic switch, Am. J. Physiol. Cell Physiol. 278 (2000) C589–C600, https://doi.org/10.1152/ajpcell.2000.278.3.C589.

[9] S. Lin, F. Brozovich, MYPT1 isoforms expressed in HEK293T cells are differentially phosphorylated after GTPγS treatment, J. Smooth Muscle Res. 52 (2016) 66–77, https://doi.org/10.1540/jsmr.52.66.

[10] P. Saldanha, I. Bolanle, T. Palmer, L. Nikitenko, F. Rivero, Complex transcriptional profiles of the PPP1R12A gene in cells of the circulatory system as revealed by in silico analysis and reverse transcription PCR, Cells 11 (2022) 2315, https://doi.org/10.3390/cells11152315.

[11] M. Irimia, R. Weatheritt, J. Ellis, N. Parikshak, T. Gonatopoulos-Pournatzis, M. Babor, et al., A highly conserved program of neuronal microexons is misregulated in autistic brains, Cell 159 (2014) 1511–1523, https://doi.org/10.1016/j.cell.2014.11.035.

[12] J. Lee, O. Villarreal, X. Chen, S. Zandee, Y. Young, C. Torok, et al., QUAKING regulates microexon alternative splicing of the rho GTPase pathway and controls microglia homeostasis, Cell Rep. 33 (2020) 108560, https://doi.org/10.1016/j.celrep.2020.108560.

[13] J. Lee, N. Lamarche-Vane, S. Richard, Microexon alternative splicing of small GTPase regulators: implication in central nervous system diseases, Interdiscip Rev RNA 13 (2022) e1678, https://doi.org/10.1002/wrna.1678.

[14] S. Anders, A. Reyes, W. Huber, Detecting differential usage of exons from RNA-seq data, Genome Res. 22 (2012) 2008–2017, https://doi.org/10.1101/gr.133744.111.

[15] M. Lopez-Abad, I. Iglesias-Platas, D. Monk, Epigenetic characterisation of CDKN1C in placenta samples from non-syndromic intrauterine growth restriction, Front. Genet. 7 (2016) 62, https://doi.org/10.3389/fgene.2016.00062.

[16] I. Iglesias-Platas, A. Martin-Trujillo, P. Petazzi, A. Guillaumet-Adkins, M. Esteller, D. Monk, Altered expression of the imprinted transcription factor PLAGL1 deregulates a network of genes in the human IUGR placenta, Hum. Mol. Genet. 23 (2014) 6275–6285.

[17] T. Schmitthen, K. Livak, Analyzing real-time PCR data by the comparative C(T) method, Nat. Protoc. 3 (2008) 1101–1108, https://doi.org/10.1093/hmg/ddu347.

[18] A. Monteagudo-Sanchez, M. Sanchez-Delgado, J. Mora, N. Santamaria, E. Gractacos, M. Esteller, et al., Differences in expression rather than methylation at placenta-specific imprinted loci is associated with intrauterine growth restriction, Clin. Epigenet. 11 (2019) 35, https://doi.org/10.1186/s13148-019-0630-4.

[19] C. Choux, P. Petazzi, M. Sanchez-Delgado, J. Hernandez Mora, A. Monteagudo, P. Sagot, et al., The hypomethylation of imprinted genes in IVF/ICSI placenta samples is associated with concomitant changes in histone modifications, Epigenetics 15 (2020) 1386–1395, https://doi.org/10.1080/15592294.2020.1783168.

[20] Z. Louadi, K. Yuan, K. Gress, O. Tsoy, O. Kalinina, J. Baumbach, et al., DIGGER: exploring the functional role of alternative splicing in protein interactions, Nucleic Acids Res. 49 (2021) D309–D318, https://doi.org/10.1093/nar/gkaa768.

[21] F. Barralle, J. Giudice, Alternative splicing as a regulator of development and tissue identity, Nat. Rev. Mol. Cell Biol. 18 (2017) 437–451, https://doi.org/10.1038/nrm.2017.27.

[22] L. Gehman, P. Stoilov, J. Maguire, A. Damianov, L. Chia-Ho, L. Shiue, et al., The splicing regulator Rbfox1 (ASBP1) controls neuronal excitation in the mammalian brain, Nat. Genet. 43 (2011) 706–711, https://doi.org/10.1038/ng.841.

[23] C. Zhang, A. Krainer, M. Zhang, Evolutionary impact of limited splicing fidelity in mammalian genes, Trends Genet. 23 (2007) 484–488, https://doi.org/10.1016/j.tig.2007.08.001.

[24] J. Khatri, Brozovich F. JoceK, S. Fisher, Role of myosin phosphatase isoforms in cGMP-mediated smooth muscle relaxation, J. Biol. Chem. 276 (2001) 37250–37257, https://doi.org/10.1074/jbc.M105275200.

[25] M. Ito, T. Nakano, F. Erdodi, D. Hartshorne, Myosin phosphatase: structure, regulation and function, Mol. Cell. Biochem. 259 (2004) 197–209, https://doi.org/10.1023/b:mcbi.0000021373.14288.00.

[26] S. Fisher, Smooth muscle phenotypic diversity: effect on vascular function and drug responses, Adv. Pharmacol. 78 (2017), https://doi.org/10.1016/bs.apha.2016.07.003, 383–41.

[27] R. Dippold, S. Fisher, A bioinformatic and computational study of myosin phosphatase subunit diversity, Am. J. Physiol. Regul. Integr. Comp. Physiol. 307 (2014) R256–R270, https://doi.org/10.1152/ajpregu.00145.2014.

[28] H. Zhang, S. Fisher, Conditioning effect of blood flow on resistance artery smooth muscle myosin phosphatase, Circ. Res. 100 (2007) 730–737, https://doi.org/10.1161/01.RES.0000260189.38975.35.

[29] S. Karim, A. Rhee, A. Given, M. Faulx, B. Hoit, F. Brozovich, Vascular reactivity in heart failure: role of myosin light chain phosphatase, Circ. Res. 95 (2004) 612–618, https://doi.org/10.1161/01.RES.0000142736.39359.58.

[30] J. Khatri, K. Joyce, F. Brozovich, S. Fisher, Role of myosin phosphatase isoforms in cGMP-mediated smooth muscle relaxation, J. Biol. Chem. 276 (2001) 37250–37257, https://doi.org/10.1074/jbc.M105275200.

[31] A. Sharp, C. Cornforth, R. Jackson, J. Harrold, A. Turner, L. Kenny, et al., Maternal sildenafil for severe fetal growth restriction (STRIDER): a multicentre, randomised, placebo-controlled, double-blind trial, Lancet Child Adolesc Health 2 (2018) 93–102, https://doi.org/10.1016/S2352-4642(17)30173-6.

[32] A. Pels, J. Derks, A. Elvan-Taspinar, J. van Drongelen, M. de Boer, H. Duvekot, et al., Maternal sildenafil vs placebo in pregnant women with severe early-onset fetal growth restriction: a randomized clinical trial, JAMA Netw. Open 3 (2020) e205323, https://doi.org/10.1001/jamanetworkopen.2020.5323.

[33] A. Khalil, A. Sharp, C. Cornforth, R. Jackson, H. Mousa, S. Stock, et al., Effect of sildenafil on maternal hemodynamics in pregnancies complicated by severe early-onset fetal growth restriction: planned subgroup analysis from a multicenter randomized placebo-controlled double-blind trial, Ultrasound Obstet. Gynecol. 55 (2020) 198–209, https://doi.org/10.1002/uog.20851.

[34] M. Payne, H. Zhang, T. Prosdocimo, K. Joyce, Y. Koga, M. Ikebe, et al., Myosin phosphatase isoform switching in vascular smooth muscle development, J. Mol. Cell. Cardiol. 40 (2006) 274–282, https://doi.org/10.1016/j.yjmcc.2005.07.009.

[35] J. Lartey, A. Gampel, J. Pawade, H. Mellor, A. Bernal, Expression of RND proteins in human myometrium, Biol. Reprod. 75 (2006) 452–461, https://doi.org/10.1095/biolreprod.105.049130.

[36] J. Lartey, M. Smith, J. Pawade, B. Strachan, H. Mellor, A. Bernal, Up-Regulation of myometrial RHO effector proteins (PKN1 and DIAPH1) and CPI-17 (PPP1R14A) phosphorylation in human pregnancy is associated with increased GTP-RHOA in spontaneous preterm labour, Biol. Reprod. 76 (2007) 971–982, https://doi.org/10.1095/biolreprod.106.058982.

[37] C. Hudson, K. Heesom, A. López Bernal, Phasic contractions of isolated human myometrium are associated with Rho-kinase (ROCK)-dependent phosphorylation of myosin phosphatase-targeting subunit (MYPT1), Mol. Hum. Reprod. 18 (2012) 265–279, https://doi.org/10.1093/molehr/gar078.

[38] A. Dordea, M. Sweeney, J. Taggart, J. Lartey, H. Wessel, S. Robson, et al., Differential vasodilation of human placental and myometrial arteries related to myofilament Ca(2+)-desensitization and the expression of Hsp20 but not MYPT1, Mol. Hum. Reprod. 19 (2013) 727–736, https://doi.org/10.1093/molehr/gat045.